C. E. Pearson and W. R. Graham: JASA Express Letters [http://dx.doi.org/10.1121/1.4904915] Published Online 31 December 2014

Experimental characterization of vertical-axis wind turbine noise

C. E. Pearson[a] and W. R. Graham
Department of Engineering, University of Cambridge, Trumpington Street, Cambridge, CB2 1PZ, United Kingdom
charlie.pearson@gmail.com, wrg11@cam.ac.uk

Abstract: Vertical-axis wind turbines are wind-energy generators suitable for use in urban environments. Their associated noise thus needs to be characterized and understood. As a first step, this work investigates the relative importance of harmonic and broadband contributions via model-scale wind-tunnel experiments. Cross-spectra from a pair of flush-mounted wall microphones exhibit both components, but further analysis shows that the broadband dominates at frequencies corresponding to the audible range in full-scale operation. This observation has detrimental implications for noise-prediction reliability and hence also for acoustic design optimization.

[SS]
Date Received: September 30, 2014 **Date Accepted:** December 8, 2014

1. Introduction

Vertical-axis wind turbines (VAWTs), with (near-)vertical blades and cylindrical swept surfaces, are insensitive to variations in wind direction; hence they are suitable for small-scale urban installations. Given this potential application, noise is an immediate concern, and one that has not yet been investigated in any depth.

The fundamental mechanisms of VAWT sound generation are described by the equation for moving bodies derived by Ffowcs Williams and Hawkings (1969). This representation identifies three contributions to the far-field noise: Thickness, arising from the missing momentum of the fluid displaced by the blades; loading, due to the blade surface stresses; and quadrupole, from non-linear sources associated with the velocities in the surrounding fluid. However, at the low Mach numbers of interest here, only the loading term is significant (Magliozzi *et al.*, 1991). Its deterministic part will generate tones at harmonics of the blade-passage frequency (BPF), while its stochastic component will give rise to broadband noise.

The deterministic aerodynamic loads on the VAWT blades can be quite reliably estimated (Howell *et al.*, 2010), so one would expect prediction of VAWT tonal noise to be relatively straightforward. The broadband component, however, is another matter because it depends on aspects of the blade flow that are much harder to model. Even in propeller applications, where the incoming flow is undisturbed and the blade operating conditions are independent of azimuth angle, broadband-noise prediction is uncertain (Magliozzi *et al.*, 1991). The significance, or otherwise, of the broadband component will thus crucially affect the ability of VAWT designers to optimize for low noise. The research reported here addresses this question.

2. Experimental method

Experiments were carried out in a low-speed wind tunnel with (hard-walled) $1.68\,\mathrm{m} \times 1.22\,\mathrm{m}$ working section and a typical free-stream turbulence intensity of

[a]Current address: Frazer-Nash Consultancy, Bristol, UK.

0.15% (Bertenyi and Graham, 2007). Measurements were taken with the 48-microphone, flush-mounted acoustic array described by Shin *et al.* (2007).

The model VAWT was constructed using off-the-shelf NHP "Razor Pro" model-helicopter rotor blades. These are manufactured from composite materials with a symmetrical aerofoil section of chord length 55 mm and maximum thickness approximately 14% of chord. The outer tip is strongly raked to provide a smooth termination that is almost square (i.e., perpendicular to the span). The inner, hub-attachment, region is tapered; this was cut off to leave a square, blunt-ended tip. The resulting blades have length 536 mm. Four were available, allowing the model to be tested in two-, three-, and four-blade configurations.

The model's shaft and spokes were made as thin as possible, subject to strength and stiffness requirements; their diameters are, respectively, 25 and 6 mm. In comparison the overall model diameter is 530 mm. The (projected) swept area of the model is thus 0.284 m^2 or 13.9% of the tunnel cross section. This is just within the range of blockage ratio (up to 14%) over which there is negligible impact on the blade aerodynamics (Howell *et al.*, 2010).

The model was installed with its shaft spanning the tunnel horizontally as shown in Fig. 1. It was viewed side-on by the (floor-mounted) acoustic array and tested at constant speed with the nearer blades traveling both with ("co-flow") and against ("contra-flow") the wind-tunnel stream. The tip-speed ratio (TSR, i.e., blade speed divided by air speed) was restricted by shaft vibration issues which limited the rotation speed to below 770 rpm. In combination with a lowest practical air speed around 4 m/s, this implied a maximum TSR of 5. Values as low as 1 were tested, but strong qualitative differences were evident in the measurements below TSR 3 in agreement with the anticipated aerodynamic working range. Hence only results for TSRs 3, 4, and 5 will be considered here. To allow direct comparison between different TSR cases, the tunnel speed was set to maintain a fixed relative air speed for a blade at its most upstream point. This speed was chosen as 21 m/s; the corresponding tunnel and rotation speeds are given in Table 1.

The microphone signals were synchronously sampled at a rate of 2048 per revolution[1] for 1200 revolutions (in the region of 100 s), yielding a total of 2 457 600 samples per channel. Individual signals are contaminated by flow "noise" (i.e., the unsteady pressure field in the tunnel-wall boundary layer). Its contribution can, however, be effectively eliminated by considering the cross-spectra between microphone

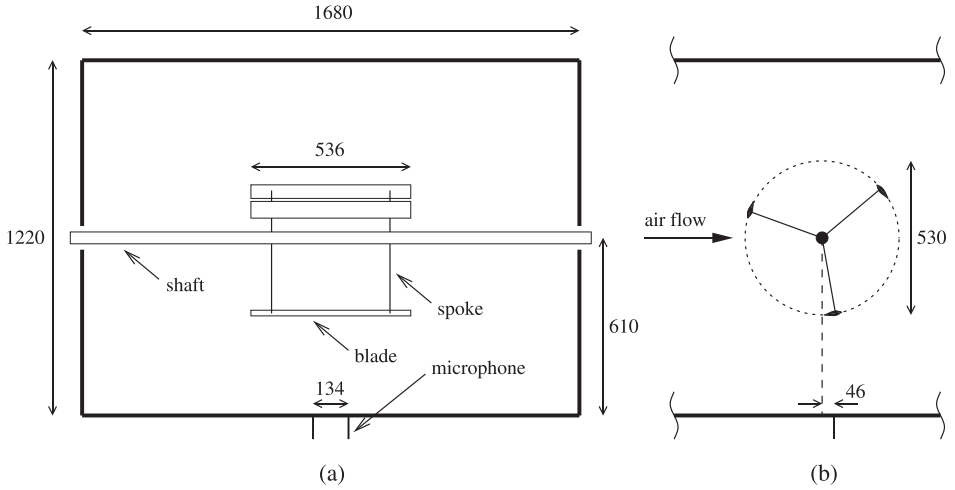

Fig. 1. The three-bladed VAWT model in the wind tunnel: (a) Tunnel cross-section view; (b) rotor axis view. The configuration shown is co-flow, corresponding to anti-clockwise rotation in view (b). All dimensions are in millimeters.

Table 1. Wind-tunnel and rotor speeds for 21 m/s relative air speed at upstream blade position.

Tip-speed ratio	3	4	5
Wind-tunnel speed (m/s)	6.6	5.1	4.1
Model-turbine rotation speed (rpm)	718	734	742

pairs. For the current question, it is sufficient to consider a single pair, which was chosen on the basis of: Proximity to the model (to maximize the acoustic contribution relative to the flow noise), separation distance (to minimize differences between the acoustic signal at each microphone), and separation direction (cross-stream, to ensure that the flow-noise contributions were effectively uncorrelated). These criteria led to microphones separated by 134 mm, located 46 mm downstream of the model axis and symmetrically either side of the tunnel center-line (see also Fig. 1). Cross-spectra were formed in the usual way from the fast Fourier transforms of the microphone signals, averaged over multiple data blocks. A Hann spatial window was employed to minimize "leakage" between spectral lines, and the data blocks were overlapped 50% to compensate for the associated weighting of different data samples.

Rejection of flow and other background noise was assessed in two ways: Consideration of spectrum convergence with increasing number of averages and comparison with measurements taken without the model but with the drive unit running at the appropriate speed. With data block size corresponding to one rotation period (2048 samples), the cross-spectra were unambiguously converged by the maximum average number (2399) and were above the associated background measurement. To differentiate between harmonic and broadband components, however, greater spectral resolution is required, and the results considered here were produced with block size 65 536. In this case, 73 averages are possible, and the noise rejection is not totally clear cut; at some local minima, the spectra are around the same level as the corresponding background measurement.

3. Results

3.1 Spectral features

Figure 2 shows the three-bladed rotor, TSR 3 cross-spectrum power for both contra- and co-flow cases. The results are plotted against rotation order (the ratio of frequency

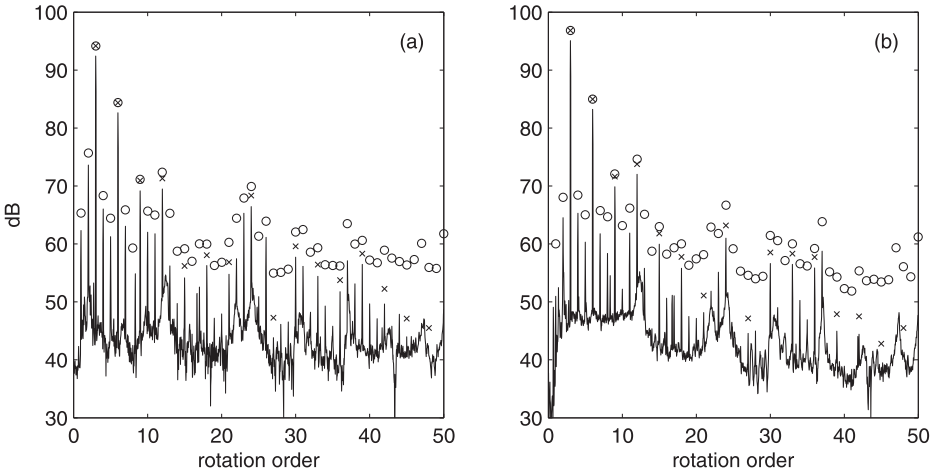

Fig. 2. Cross-spectrum power (in dB referred to 4×10^{-10} Pa^2) for the three-bladed rotor operating at TSR 3 in (a) contra-flow, and (b) co-flow, configurations. Symbols: ○, total power in rotation order "bin"; ×, tonal power at BPF harmonics.

to rotation speed); harmonic components are expected at orders 3, 6, 9, etc., in this case. Sharp peaks at these points are indeed evident; however, other rotation-order harmonics are also visible at lower levels. Similar peaks are found in the background-noise measurements (due to the drive unit), but some of the ones here are higher and therefore must arise from slight mismatches between the individual blade contributions. Finally, broader peaks are evident at rotation orders beyond 10; these were found to be flow-speed invariant, and hence are associated with the duct resonances of the wind tunnel.

Also shown in the plots of Fig. 2 are circular symbols at integer values of the rotation order. These represent the cross-spectrum power in a frequency "bin" of width equal to the rotation rate (12.0 Hz in this case) and can be compared directly to the harmonic peaks. Ideally, if the spectrum were harmonic-dominated, they would coincide. In practice, however, even a pure harmonic is "smeared" by data windowing, and detailed examination of the peaks here shows that they consist of a maximum at the integer rotation order, flanked by a pair of points around 6 dB lower. The crosses plotted at BPF orders correspond to the sums of these three values only. A direct comparison of the crosses with the bin-power symbols then leads to the conclusion that effectively all the sound at rotation orders 3 and 6 is harmonic and that broadband contributions gradually become significant thereafter. Note that this conclusion is robust to the caveat of Sec. 2 regarding convergence because the bin powers are calculated by summing the *complex* individual contributions rather than their magnitudes. The frequency-domain averaging implicit in this approach is equivalent to performing the original analysis with smaller block length (in this case the 2048-sample instance for which convergence was checked and confirmed).

3.2 Parametric dependence of harmonic noise

The tonal contributions that are predictable on the basis of deterministic blade-force calculations are those at BPF harmonics only. Therefore to gauge the extent of their dominance, they must be compared against the total cross-spectrum power in a blade-passage, rather than rotation-frequency, bin. For the example of Fig. 2, this entails comparing each cross against the sum of the associated circle symbol and its immediate neighbors. The results are presented in Figs. 3(b) and 4(b) as ratios of harmonic to bin power for the contra- and co-flow cases. Also shown in these plots are the corresponding results at TSRs 4 and 5. Similarly, Figs. 3(a)/4(a) and 3(c)/4(c) show the

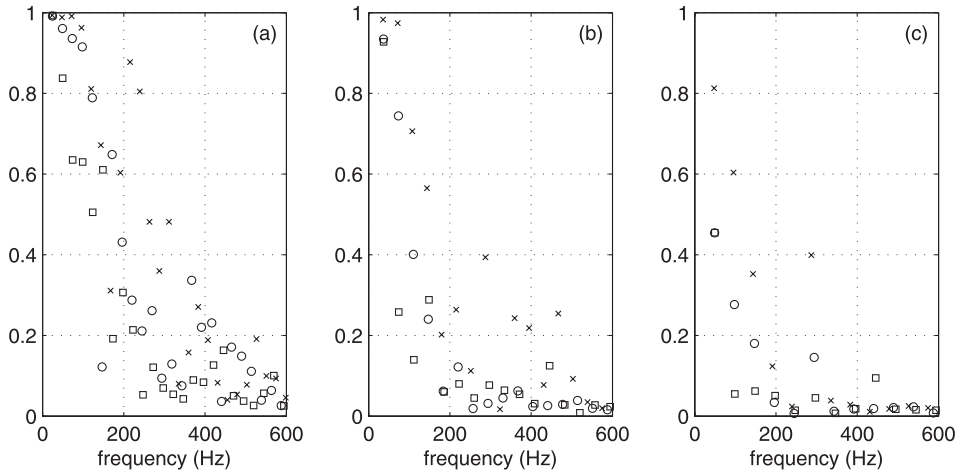

Fig. 3. Ratios of tonal power at BPF harmonics to overall power in corresponding frequency bins for the contra-flow configuration: (a) Two-bladed rotor; (b) three-bladed rotor; (c) four-bladed rotor. Symbols: ×, TSR 3; ○, TSR 4; □, TSR 5.

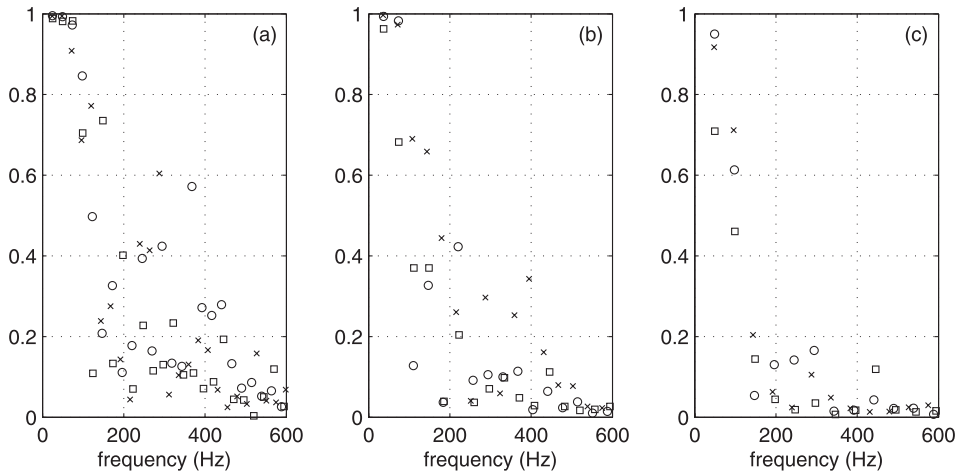

Fig. 4. Ratios of tonal power at BPF harmonics to overall power in corresponding frequency bins for the co-flow configuration: (a) Two-bladed rotor; (b) three-bladed rotor; (c) four-bladed rotor. Symbols: ×, TSR 3; ○, TSR 4; □, TSR 5.

contra- and co-flow power ratios for, respectively, the two- and four-bladed rotors at all three TSRs. Note that even at the same TSR, the blade-passage frequency varies with blade number, so the abscissae show frequency rather than harmonic order. The range corresponds to that of Fig. 2.

Although there are some detail differences, both contra- and co-flow results exhibit consistent trends with blade number and with TSR. The clearest are the former; as blade number increases, there is a marked reduction in the higher-harmonic contribution. Even the lower harmonics are affected to some extent; compare, for instance, the first blade-passage tone data for the four-bladed rotor with that for the two-bladed case (or, to match frequencies, the two-bladed second blade-passage tone). Increasing TSR appears to have a similar effect; in general, the relative significance of any given harmonic tends to drop. However, this observation is not universal, especially for those orders whose contribution is small compared to the total bin power.

Finally, Figs. 3 and 4 yield the overall conclusion that, almost without exception, the blade-passage-harmonic contribution represents under half the acoustic power at frequencies above 250 Hz. (The two anomalies are both for the two-bladed, co-flow case, for TSR 3 at 287 Hz and TSR 4 at 368 Hz.) The implications for full-scale VAWT noise are discussed in Sec. 4.

4. Discussion

The results presented here are robust to the modifying effect of modal behavior in the wind tunnel because the frequency bins are narrow in comparison to the duct-resonance peaks. Nonetheless, they cannot be extrapolated to full-size VAWTs without consideration of two further issues. The first is that of Reynolds-number effects. The experimental blade speed of 21 m/s is representative of full scale; it would correspond to a TSR of 4.7 at a typical cut-on wind speed of 4.5 m/s (Microstrain, 2014). The blade chord is smaller though, so the experimental Reynolds number (7.7×10^4) is low. This is a common problem in experimental aerodynamics, but one that is typically found to have only a weak effect on lifting forces. Because it is these forces that (necessarily) dominate in the design operating regime for a VAWT, it is tempting to dismiss the Reynolds-number question without further consideration. Note, however, that the experimental condition is not quite at the "super-critical" value where this argument is legitimate (Simons, 1994). Hence some difference in (dimensionless) force coefficients is to be expected but in the direction of increased harmonic content in the experiments.

This claim is based on the greater susceptibility of aerofoils to stall at lower Reynolds numbers, and the expectation (supported by the results shown here, and also tests at lower TSRs) that the rapid force changes associated with stall will increase the bandwidth of the deterministic blade-force record.

The second question is a simpler one: What are the full-scale frequencies corresponding to the measured values? These can be deduced from the reference speed and the 3.1 m diameter of a (three-bladed) full-scale exemplar (Microstrain, 2014); the rotation frequency is then 2.2 Hz and the BPF 6.5 Hz. Hence the tenth BPF tone, above which broadband noise dominates, is at 65 Hz, barely in the audible range, and certainly well outside the region of high sensitivity. Thus although perceived noise cannot definitively be predicted on the basis of spectra alone, it appears likely that tonal contributions will be irrelevant for full-scale VAWTs.

5. Summary

This work has addressed the relative importance of broadband and harmonic components in vertical-axis wind turbine noise, via model-scale wind-tunnel experiments. Cross-spectrum measurements from a pair of wall-mounted microphones show that, at full scale, the broadband contribution will dominate in the audible range, and hence that the harmonics are unlikely to affect the perceived noise. This complicates the acoustic design and optimization task.

Acknowledgments

The first author thanks the UK Engineering and Physical Sciences Research Council for a Doctoral Training Grant. Support for the experiments was provided by Quiet Revolution Ltd.

Reference and links

[1]The acquisition hardware provides the 2048 samples by averaging data from a 100 kHz stream to produce a subsampled set with near-uniform time spacing. Uniformly spaced records were generated, via linear interpolation, as the first post-processing step.

Bertenyi, T., and Graham, W. R. (**2007**). "Experimental observations of the merger of co-rotating wake vortices," J. Fluid Mech. **586**, 397–422.
Ffowcs Williams, J. E., and Hawkings, D. L. (**1969**). "Sound generation by turbulence and surfaces in arbitrary motion," Philos. Trans. R. Soc. London A **264**, 321–342.
Howell, R., Qin, N., Edwards, J., and Durrani, N. (**2010**). "Wind tunnel and numerical study of a small vertical axis wind turbine," Renewable Energy **35**, 412–422.
Magliozzi, B., Hanson, D. B., and Amiet, R. K. (**1991**). "Propeller and propfan noise," in Aeroacoustics of Flight Vehicles: Theory and Practice, NASA RP1258, edited by H. H. Hubbard (National Aeronautics and Space Administration, Washington, DC), Vol. 1.
Microstrain (**2014**). "Product specification and power curve," *QR5 Quietrevolution Turbine*, http://www.microstrain.ie/quietrevolution.html (Last viewed September 30, 2014).
Shin, H. C., Graham, W. R., Sijtsma, P., Andreou, C., and Faszer, A. (**2007**). "Implementation of a phased microphone array in a closed-section wind tunnel," AIAA J. **45**, 2897–2909.
Simons, M. (**1994**). *Model Aircraft Aerodynamics*, 3rd ed. (Argus, Hemel Hempstead, UK).